# Experimental Report

**Proposal title :** Liquid crystal topological defects at the nanoscale precision
**Proposal number :** SC-5368
**Beamline :** ID01
**Shifts :** 12
**Date(s) of experiment :** from 30/03/2023 to 03/04/2023
**Date of report :** 05/10/2023
**Local contact :** Peter BOESECKE

## Objective and expected results

We study 4-n-octyl-4'-cyanobiphenyl (8CB) smectic A liquid crystal (LC) films, either pure thin films or composites thin films with nanoparticles (NPs). The LC film is characterized by an antagonist anchoring at the two interfaces because the 8CB smectic layers are perpendicular to the substrate (glass substrate with 10nm of rubbed PVA polymer) with their normal fixed along the rubbing of the polymer and parallel to the 8CB-air interface. This hybrid anchoring leads to an original texture called "oily streaks" where the Sm layers are curved into flattened hemicylinders oriented along a single direction (Figure 1b) [1]. The width of the flattened hemicylinders, in the range 400 nm-800 nm, depends on the LC film thickness. The flattened hemicylinders can be detected by Polarized Optical Microscopy (POM – Figure 1a). By combining POM, ellipsometry and X-ray diffraction performed on SIXS Soleil beamline, we have shown that these oily streaks are characterized by the presence of 3 kinds of coexisting topological defects (TDs) : dislocations - in purple on Figure 1b, disclinations - in red on Figure 1b, and central 2D grain boundary - in green on Figure 1b [1]. A number of theoretical works have predicted the LC defect core characteristics, the elastic features outside the core, etc... [2]. However almost no experimental work is yet able to determine the nanoscale structure of these defects. For smectic dislocations as an example, only one TEM measurement for smectic C materials is available [3] and one POM measurement for giant smectic rods made of viruses [4]. Moreover, it is known that LC TDs, of core size expected to be of the same order than NP size, attract and confine NPs in the defect cores, thus playing the role of new kinds of template to achieve original NP assemblies [5-7].

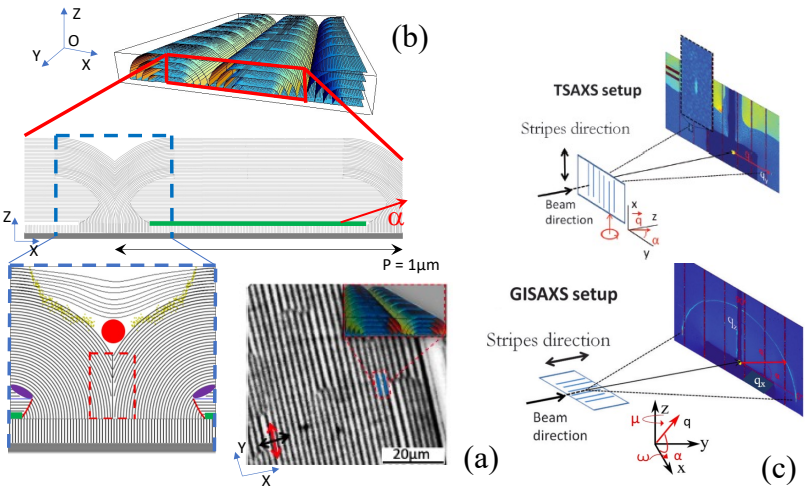


Figure 1 – a) POM image of smectic film observed between crossed polarisers b) with the corresponding model of the smectic oily streaks in flattened hemicylinders. The Cross-sectional view of one oily streak hemicylinder is shown with rotating grain boundary (red lines), linear dislocations (purple dots), disclinations (red dot) and 2D topological grain boundary (green). c) the two set-up that are used are the GI-SAXS set-up and the TSAXS set-up

It is consequently of interest to study the nanoscale features of LC TDs, revealing their core size but also the elastic distortion around the core, both for pure samples and for LCs with NPs confined in the

TD cores and to study the NP organization in relation with the defect characteristics.

We have thus performed a first test of nano-diffraction at the ESRF beamline ID01. The idea was to scan the sample with a beam of size around 60nm and record the scattered intensity during the scanning. In particular a scan perpendicular to the hemicylinders (Ox direction in Figure 1) might allow for localized measurements of the defects themselves or of the nanoparticle assemblies in relation with the defects structure. The test unfortunately appeared to be shortened due to technical problems the first day, thus leading to only 48 hours of measurements. We have mostly measured pure 8CB liquid crystal films in TSAXS and GISAXS (Figure 1c) and, using the GISAXS set-up, composite liquid crystal films with small gold nanospheres a priori included in both the central 2D grain boundaries (in green in Figure 1b) and in the 1D defects, dislocations and disclinations (in purple and red in Figure 1b). A crucial question was to understand if it was indeed possible to detect the scattering of the smectic layers and of the nanoparticles organized in the smectic defects, despite the high brillance of EBS-ESRF.

# Results and conclusions of the study

## 0.1 Pure LC thin film :

Figure 1c shows the GISAXS setup. With this set-up we obtained the 8CB scattering shown on Figure 2 for a 200 nm 8CB film, with the beam parallel to the hemicylinders. It appears similar to the one that was obtained for an average measurement at Soleil (Figure 1c). This confirms that, despite the very high brilliance, we could correctly measure the scattering of these smectic liquid crystals at ESRF. This signal appeared to be stable for several minutes without any radiation damage, which is encouraging for future measurements. However, after 20 minutes of scanning over areas as small as $10\mu m \times 10\mu m$, systematically almost all the 8CB film covering an area of $18mm \times 18mm$ had evaporated. This suggests that the irradiation dose is the crucial parameter for the comportment of the overall sample under X-ray beam. Fast experiments will thus be necessary in the future. They will require to enhance the signal to noise ratio through an accurate configuration of the beamstop. This last feature will also be necessary to improve the TSAXS measurements. We could only reveal the TSAXS signal once on a very localized area, most probably on a locally thicker (and less well-oriented) area. The fact that the entire hemicylindrical signal appears with a beam as small as 60nm (Figure 2) also suggests that the 8CB hemicylinders are not perfectly straight in the beam footprint of around 10 $\mu m$. We will thus work for the next experiment on the regularity of the smectic hemicylinders in the beam to produce hemicylinders that would be perfectly straight along more than $10\mu$m. This is clearly possible through an accurate control of the anchoring strength provided by our rubbing machine.

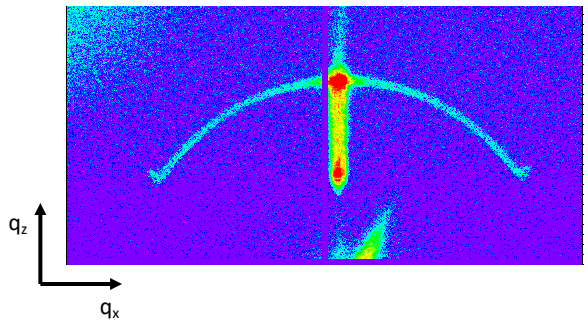


Figure 2 – Scattering of the rotating smectic layers at the edges of the hemicylinders.

## 0.2 LC/NP composite film :

The organization of gold nanospheres has also been successfully measured with the X-ray beam width as small as 60 nm. Gold nanospheres with a radius of 3 nm were embedded in a 180 nm thick LC film. The formation of a 2-dimensional hexagonal network [7] is shown on the three top pictures of Figure 3a through the two scattering rods (arrows on Figure 3a). A GISAXS scan perpendicular to the direction of the hemicylinders at a nanoscale is necessary to obtain separate information from the different defects zones of the hemicylinders. When scanning the sample in the direction perpendicular to the hemicylinders (perpendicular to the stripes identified by optical Microscoy - figure 1a) we see the

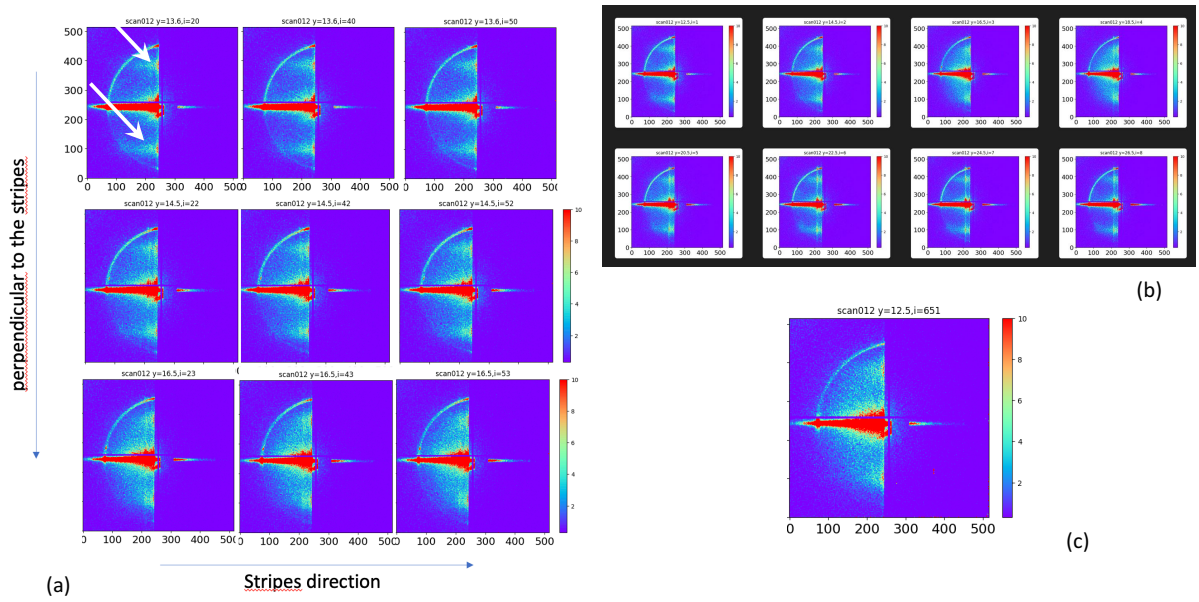


FIGURE 3 – (a) evolution of the scattering of the gold nanospheres during the 2D scanning : The scanning perpendicular to the hemicylinders is along the three columns, the three columns being at three different positions along the smectic hemicylinders. The three top pictures display two rods, shown by arrows, associated with the presence of hexagonal networks of gold nanospheres.(b) Exemple of longer perpendicular scanning. (c) typical detector picture at the end of the 2D scan.

evolution of the scattering rods signal in the three columns of figure 3a, each column being at different position along the hemicylinders. The evolution is characterized by scatterings rods (three top pictures of figure 3a) that almost disappear during the scanning (three bottom pictures of figure 3a). This can be interpreted by the transformation from the signal of hexagonal networks of nanospheres formed in the central topological defect of the hemicylinder (in green in Figure 1b) to chains of nanospheres formed in the 1-dimensionnal defects of the edge of the hemicylinder (disclination in red and dislocation in purple of Figure 1b). The stability of the scattering observed in the perpendicular direction (parallel to the stripes identified by optical Microscopy - figure 1a) agrees with the expected hemicylindrical geometry of the liquid crystal. Figure 3b shows that for one specific position in the hemicylinder, extensive perpendicular scanning leads to a recovering of the rods (5th to 7th picture in Figure 3b) related to the hexagonal network after detection of the nanosphere chain signal (4th picture in Figure 3b). This can be interpreted by a measurement of the center of the second neighbouring hemicylinder after having scanned a first hemicylinder. Unfortunately we have scanned the sample in steps of 2 microns in the direction perpendicular to the hemicylinders and in steps of 100 nm in the direction of the hemicylinders due to an error on the two axes parallel to the substrate in the GISAXS set-up, preventing any fine quantitative tuning of the nanosphere organization. We have anyway demonstrated the feasability of the nanoscale analysis of the assembly of nanoparticles confined in the LC topological defects.

2D scan were performed for repeatability purposes and to assess the radiation damages. We scanned a 20 $\mu$m x 10 $\mu$m area during 500 s. No variation along the hemicylinders occured during the first seconds of measurements as shown on Figure 3a (comparison between the various columns) but systematically the last scans perpendicular to the hemicylinders displayed everywhere the same scattering of single nanospheres with not any scattered rod anymore (Figure 3c). The picture of Figure 3c is similar to the three bottom pictures of figure 3a and to the 4th picture of Figure 3b in agreement with the fact that the scattering of nanosphere chains parallel to the X-ray beam is expected to be similar to the one of single nanospheres. The radiation damages were evidenced after the first 100 images (50s) suggesting that gold NPs are more affected by radiation damages than smectic LC.

## 0.3 Conclusion

In conclusion, during these 48 hours of test measurements at ID01, we successfully measured the X-ray scattering signal associated with 8CB smectic layers superimposed into flattened hemicylinders. We also measured the scattering of gold nanosphere assemblies confined in the smectic topological defects AND

its expected variations during a scanning perpendicular to the smectic hemicylinders. These encouraging results deserve now accurate and extensive measurements of both pure LC and of composites with nanospheres of various sizes and with nanorods. These future measurements will require a careful adjustment of the beamstop, a close attention to the effects of radiation damages and the building of 8CB hemicylinders that would be perfectly straight along more than $10\mu$m. This will allow for a study of the different zones of smectic defects independently. A determination of both defect cores and elastic distortion around the cores will become possible. The specific structural determination of the NP assemblies within each specific defect will also become possible allowing for a fine study of the interaction between topological defects and NPs.

## Références


[1] Delphine Coursault et al. "Self-organized arrays of dislocations in thin smectic liquid crystal films". In : *Soft Matter* 12.3 (2016), p. 678-688.

[2] H. Aharoni, T. Machon et R. D. Kamien. "Composite Dislocations in Smectic Liquid Crystals". In : *Phys. Rev. Lett.* 118 (2017), p. 257801.

[3] C Zhang et al. "Nanostructure of edge dislocations in a smectic-C ? liquid crystal." In : *Phys Rev Lett.* 115 (2015), p. 087801.

[4] A Repula et E. Grelet. "Elementary edge and screw dislocations visualized at the lattice periodicity level in the smectic phase of colloidal rods." In : *Phys Rev Lett.* 121 (2018), p. 097801-097801.

[5] Delphine Coursault et al. "Linear self-assembly of nanoparticles within liquid crystal defect arrays". In : *Advanced Materials* 24.11 (2012), p. 1461-1465.

[6] Delphine Coursault et al. "Tailoring anisotropic interactions between soft nanospheres using dense arrays of smectic liquid crystal edge dislocations". In : *ACS nano* 9.12 (2015), p. 11678-11689.

[7] Syou-Pâheng Do et al. "From Chains to Monolayers : Nanoparticle Assembly Driven by Smectic Topological Defects". In : *Nano letters* 20.3 (2020), p. 1598-1606.